

Lawrence Berkeley National Laboratory

LBL Publications

Title

Spatially resolved characterization of electromigration-induced plastic deformation in al (0.5wt% cu) interconnect

Permalink

<https://escholarship.org/uc/item/1mt2r1p2>

Author

Spolenak, R.

Publication Date

2003

**SPATIALLY RESOLVED CHARACTERIZATION OF
ELECTROMIGRATION-INDUCED PLASTIC DEFORMATION IN AL
(0.5WT% CU) INTERCONNECT**

R.I. Barabash and G.E. Ice

Metals & Ceramics Divisions, Oak Ridge National Laboratory, Oak Ridge TN 37831

N. Tamura and J.R. Patel

Advanced Light Source, 1 Cyclotron Road, Berkeley CA 94720

B.C. Valek and J. C. Bravman

Dept. Materials Science & Engineering, Stanford University, Stanford CA 94305

R. Spolenak

Max Planck Institut für Metallforschung, Heisenbergstrasse 3, D-7056 Stuttgart, Germany

ABSTRACT

Electromigration during accelerated testing can induce large scale plastic deformation in Al interconnect lines as recently revealed by the white beam scanning X-ray microdiffraction. In the present paper, we provide a first quantitative analysis of the dislocation structure generated in individual micron-sized Al grains during an in-situ electromigration experiment. Laue reflections from individual interconnect grains show pronounced streaking after electric current flow. We demonstrate that the evolution of the dislocation structure during electromigration is highly inhomogeneous and results in the formation of unpaired randomly distributed dislocations as well as geometrically necessary dislocation boundaries. Approximately half of all unpaired dislocations are grouped within the walls. The misorientation created by each boundary and density of unpaired individual dislocations is determined.

INTRODUCTION

During service, the tiny Al or Cu metallic interconnect lines which connect discrete components in modern integrated circuits, experience extremely high current densities on the order of 1 MA/cm². The so-called electron “wind” force is sufficient to “physically” displace the constitutive atoms in the interconnect lines. This phenomenon, called electromigration, depletes material at the cathode end of the interconnect line and cause accumulation near the anode end¹. Ultimately electromigration leads to failure by open- (void and hillock formation) or short- (cracking of the passivation layer and material extrusion) circuit (Fig.1). Electromigration-induced failure in metal interconnect constitutes a major and growing reliability problem in the semiconducting industry². While the general mechanism of electromigration is understood³, the effect of the atomic flow on the local metallic line microstructure is largely unknown.

Recently, experimental techniques capable of probing grain orientation and stress with a spatial resolution compatible with the dimensions of the lines have emerged⁴⁻¹². White beam X-ray microdiffraction⁴⁻⁸ is particularly well suited to the *in-situ* study of

electromigration. The technique was used to probe microstructure in interconnects^{4,13-16} and recently unambiguously unveiled the plastic nature of the deformation induced by mass transport during electromigration in Al(Cu) lines¹⁷.

The aim of the present paper is to understand the complex dislocation structure arising from electromigration-induced plastic deformation by simulating the shape of the reflections observed in the experimental data. Custom software allows us to determine the orientation of the predominant dislocation network in each sample subgrain^{18,19}.

EXPERIMENTAL DETAILS

Data collection has been carried out on the X-ray microdiffraction end station (7.3.3.) at the Advanced Light Source. The sample is a patterned Al(0.5% wt. Cu) line (length: 30 μm , width 4.1 μm , thickness 0.75 μm) sputter deposited on a Si wafer and buried under a glass passivation layer (0.7 μm thick). Electrical connections to the line are made through unpassivated Al(Cu) pads connected to the sample by W vias. The sample was maintained at a constant temperature of 205 °C and the current density was progressively ramped up to 0.98 MA/cm² and maintained at this value for a period of 11 hours. The direction of the current was then reversed for a total period of 19 hours. Before and during the course of electromigration, the sample was repeatedly raster-scanned under a micron-size white beam with a step size of 0.5 μm . At each step, a CCD diffraction frame was collected. Each scan contains 975 frames covering the total surface of the sample. In the present paper, we concentrate on the evolution of the diffraction pattern of one particular grain (Grain A, size: \sim 2.5 μm) situated approximately half-way between the middle of the line and the anode end. Details on the experimental setting and data collection can be found elsewhere⁴⁻⁶. A qualitative description and semi-quantitative interpretation of the entire data set collected for the present sample can be found in a recent article¹⁷. Orientation maps obtained from the x-ray microdiffraction scans reveal that the grain structure of the line has a random in-plane orientation and pronounced (111) fiber texture. Only one or a few grains span the line (near bamboo configuration). Grain A is in a region of the line, where multiple grains are found transverse to the line.

RESULTS AND DISCUSSION

The white beam CCD frames show sharp Laue reflection before electromigration and pronounced streaking of the Laue reflections in the majority of Al grains after electric current flow (Fig.2). The average streaking direction is approximately transverse to the length of the line (and not along the line). Intensity distributions along the streak direction (ξ) are typically non-uniformly bunched into several maxima indicating that the dislocation distribution is inhomogeneous. The dislocation structure was analyzed based on the approach described by Barabash et al.^{18,19}. Here we extended the method to consider individual unpaired dislocations (GNDs for Geometrically Necessary Dislocations) within the scattering domains separated by geometrically necessary dislocation boundaries (GNBs).

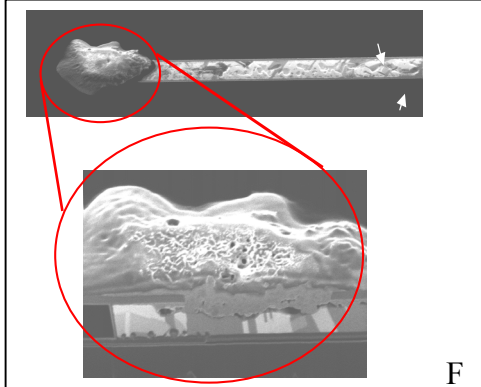


Fig.1. Focused Ion Beam (FIB) image after electromigration test of a Cu line showing a large hillock and local damages

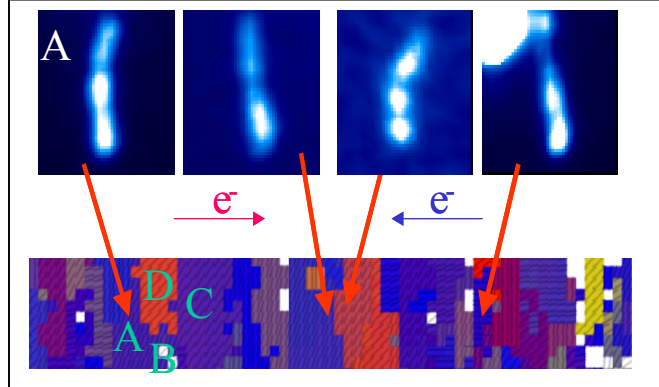


Fig.2. Experimental streaking of Laue images for different grains of interconnect line in a bamboo region.

Consider a net of individual unpaired edge dislocations with a density n^+ within interconnect (Fig.3). All dislocations from this set have Burgers vectors, \mathbf{b}_i and dislocations lines τ . We introduce a coordinate system with the X axis in the direction of the Burgers vector and the Z-axis in the direction of the dislocation line. Each edge dislocation in the XY plane creates a displacement \mathbf{u}_{it} of the i -th scattering cell in that plane. The total displacement of the i -th cell \mathbf{u}_i is due to all dislocations¹⁹ $\mathbf{u}_i = \sum_t c_t \mathbf{u}_{it}$.

For our net of parallel unpaired dislocations, the mean deformation tensor $\hat{\omega}^r$ has only two non-zero components $\omega_{xy}^r = -\omega_{yx}^r = n^+ b x$. This distortion field represents a pure rotation about the Z axis that increases with displacement in x . To take into account the presence of geometrically necessary tilt boundaries we consider several GNBs formed by walls of edge dislocations¹⁹⁻²¹. The mean deformation tensor ω^w due to the presence of tilt GNBs results in pure rotations about the direction of dislocation lines in the wall. For the orientation of the dislocations within a wall described above, an axis X is perpendicular to the plane of the wall, and an axis Z parallel to the direction of dislocation lines in the wall. Local lattice rotation fields from individual dislocations and GNBs superimpose and the mean distortion field tensor can be written as follows $\omega_{xy} = \omega_{xy}^w + \omega_{xy}^r$.

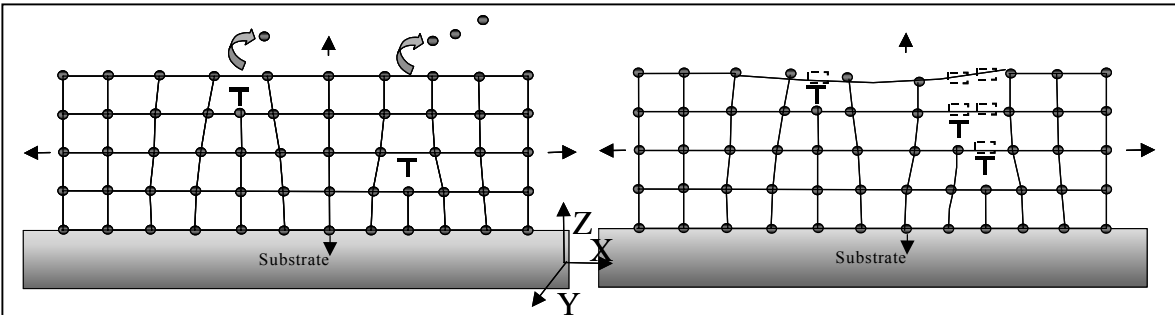


Fig. 3. Scheme of dislocation climb and formation of vacancies, unpaired random dislocations (left) and dislocation wall (right) during electromigration.

Near a Laue reflection, we can define two natural axes ξ and ν in the plane perpendicular to the momentum transfer unit vector \mathbf{g} . As in reference [18,19] with this co-ordinate system, the diffuse scattering is strongly elongated in the ξ direction. The full width at half maximum in the ξ direction, FWHM_ξ depends on the average distance between GNBs, their mutual orientation with the momentum transfer G , the type of GNB (tilt or twist), and the incident x-ray beam direction.

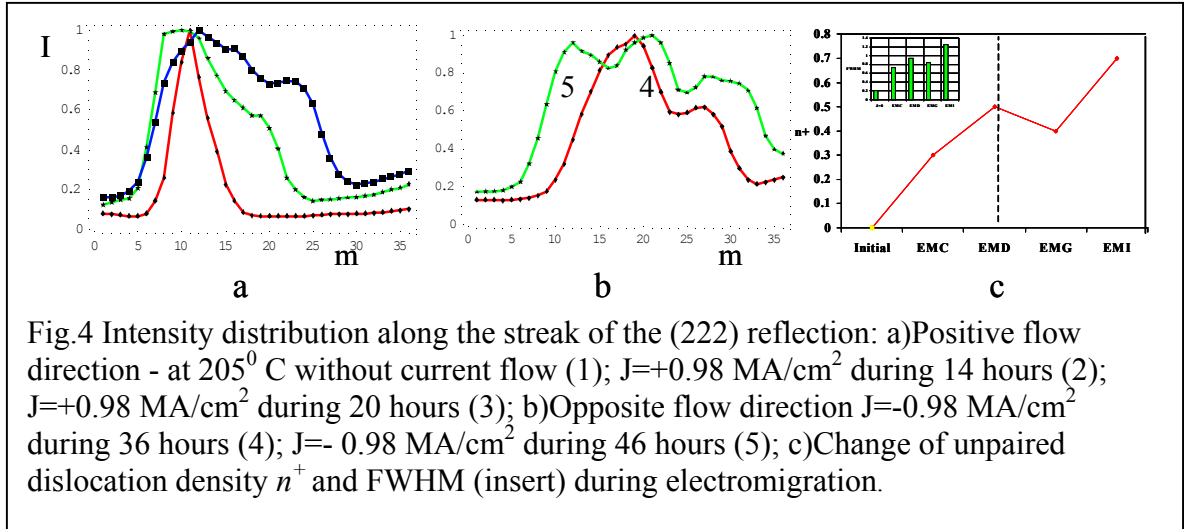


Fig.4 Intensity distribution along the streak of the (222) reflection: a) Positive flow direction - at 205⁰ C without current flow (1); $J=+0.98 \text{ MA/cm}^2$ during 14 hours (2); $J=+0.98 \text{ MA/cm}^2$ during 20 hours (3); b) Opposite flow direction $J=-0.98 \text{ MA/cm}^2$ during 36 hours (4); $J=-0.98 \text{ MA/cm}^2$ during 46 hours (5); c) Change of unpaired dislocation density n^+ and FWHM (insert) during electromigration.

Stereographic projections of all Laue spots in (111) plane were recovered from experimental data. The intensity profiles along the streak at different times during the electromigration process are presented in Fig. 4a for grain A in the reciprocal space. Continuous streaks are observed near all Laue spots in the first measurements made at 0.98 MA/cm² (Fig.4b, curve 1). The full width at half maximum (FWHM_ξ) along the streak direction increased almost twice relatively to the initial (no current) state (Fig. 4a, curve 2). The highly asymmetric shape of the intensity profile along the streak indicates that the arrangement of unpaired dislocations is inhomogeneous. The orientation of the primary unpaired (geometrically necessary) dislocations (GND) corresponds to a Burgers vector $\mathbf{b}=[0-11]$ and a dislocation line direction $\tau=[2-1-1]$. The density of unpaired dislocations is equal to $n^+ = 0.3 \cdot 10^{10} \text{ cm}^{-2}$ (Fig.4c), which is a quite reasonable value for plastically deformed Al. After 6 additional hours at the same current density, the intensity distribution breaks into two distinct maxima (Fig.4a, curve 3) indicating that the dislocation structure partially relaxed with the formation of a geometrically necessary boundary (GNB). The misorientation created by this boundary is $\sim 0.38^\circ$. The average distance between the boundary dislocations within the wall is estimated to be 430Å. The density of boundary dislocations is about $0.3 \cdot 10^{10} \text{ cm}^{-2}$. The FWHM_ξ along the streak direction within each maximum again increased (Fig.4a, curve 3). The density of unpaired individual dislocations within each scattering domain at this stage is equal to $n^+ = 0.5 \cdot 10^{10} \text{ cm}^{-2}$ (Fig.4c).

We then reversed the direction of the current flow to -0.98 MA/cm² and after 6 hours the total FWHM_ξ of the streaks decrease slightly (Fig.4b, curve 4). This indicates that the opposite direction of the current may “cure” some part of randomly distributed unpaired individual dislocations. The density of unpaired individual dislocations within each

scattering domain slightly decreases to $n^+ = 0.4 \cdot 10^{10} \text{ cm}^{-2}$. However, the dislocations being grouped into a sub-boundary form a very stable arrangement, which are not destroyed by the opposite direction of the current. Its misorientation remains practically the same as in previous stage boundary and is equal to 0.38° . After 10 hours with $J = -0.98 \text{ MA/cm}^2$ a second sub-boundary with $\mathbf{b}=[110]$, $\tau=[-112]$ is generated. The FWHM_ξ of the streak again almost doubled and three distinct maxima are observed (Figs.4b, curve 5). The second geometrically necessary boundary creates misorientation of 0.52° around the $[\bar{1}12]$ axes. The average distance between the boundary dislocations within the wall decreases to 315 \AA . The total density of boundary dislocations within the above two boundaries is equal to $0.7 \cdot 10^{10} \text{ cm}^{-2}$. Approximately half of all unpaired dislocations remain randomly distributed within the three fragments with a density of $0.7 \cdot 10^{10} \text{ cm}^{-2}$. We have simulated the Laue images (contourmaps) corresponding to the experimental dislocation arrangements. In Fig.5, the best fits are shown for (313) and (224) reflections.

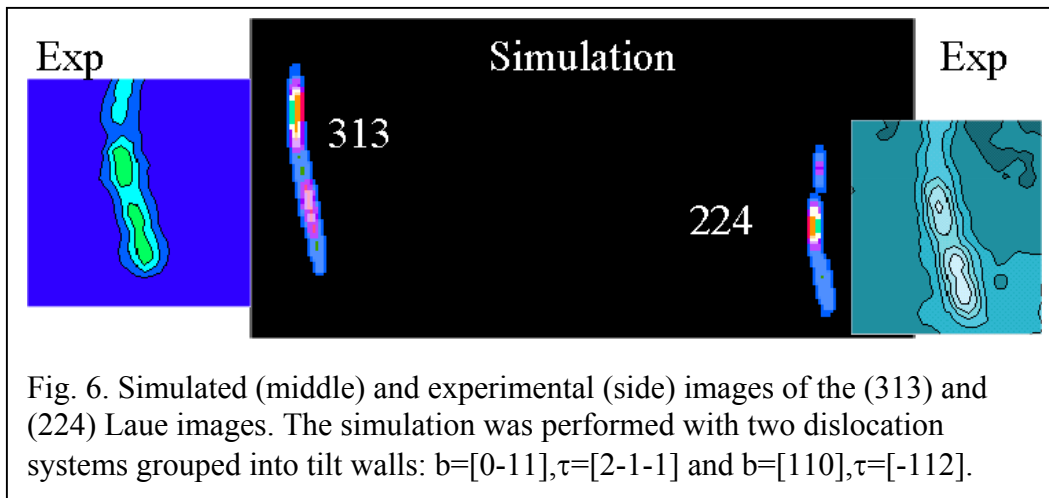


Fig. 6. Simulated (middle) and experimental (side) images of the (313) and (224) Laue images. The simulation was performed with two dislocation systems grouped into tilt walls: $\mathbf{b}=[0-11]$, $\tau=[2-1-1]$ and $\mathbf{b}=[110]$, $\tau=[-112]$.

Our analysis of the orientation of the activated dislocation slip systems shows that the slip systems with dislocation lines almost parallel to the direction of current flow are activated first. While the possibility of plastic yield during electromigration has been considered in the literature³, a direct quantitative analysis of the dislocation formation during electromigration is performed here for the first time.

ACKNOWLEDGEMENT

Research is supported by the Director, Office of Science, Office of Basic Energy Sciences, U.S. Department of Energy, under Contract DE-AC05-00OR22725 with UT-Battelle, LLC and with the Advanced Light Source, Materials Science Division, under the Contract No. DE-AC03-76SF00098 at Lawrence Berkeley National Laboratory.

REFERENCES

- ¹ I.A. Blech, J. Appl. Phys., **47**, 1203 (1976).
- ² C.V. Thompson and J.R. Lloyd, Mater. Res. Soc., Bull. **18**, 19 (1993).
- ³ M.A. Korhonen, P. Borgesen, K.N. Tu, and C.-Y. Li, J. Appl. Phys. **73**, 3790 (1993).

- ⁴N. Tamura, A.A. MacDowell, R.S. Celestre, H.A. Padmore, B.C. Valek, J.C. Bravman, R. Spolenak, W.L. Brown, T. Marieb, H. Fujimoto, B.W. Batterman and J.R. Patel, *Appl. Phys. Lett.* **80** (2002) 3724-3727.
- ⁵N. Tamura; R. Spolenak, B.C. Valek; A. Manceau; M. Meier Chang; R.S. Celestre; A.A. MacDowell; H.A. Padmore and J.R. Patel; *Review of Scientific Instruments* **73** (2002) 1369-1372.
- ⁶A.A. MacDowell, R.S. Celestre, N. Tamura, R. Spolenak, B.C. Valek, W.L. Brown, J.C. Bravman, H.A. Padmore, B.W. Batterman and J.R. Patel, *Nuclear Instruments and Methods in Physics Research A* **467-468** (2001) 936-943
- ⁷G.E. Ice and B. C. Larson, *Advanced Engineering Materials*, (2002), **2**,10, 643-646
- ⁸B.C. Larson, Wenge Yang, G.E. Ice, J.D. Budai and J.Z. Tischler, *Nature*, (2002), **415**, 887-890
- ⁹L. Margulies, G. Winther and H.F. Poulsen, *Science*, (2001) **291**, 2392-2394
- ¹⁰J.S. Chung, G.E. Ice, *J. Appl. Phys.*, (1999) **86**, 9, 5249-5255.
- ¹¹P.-C. Wang, I. C. Noyan, S. K. Kaldor, J. L. Jordan-Sweet, E. G. Liniger, and C.-H. Ku, *Appl. Phys. Lett.*, **78**, 2712 (2001).
- ¹²P. C. Wang, G. S. Cargill III, I. C. Noyan and C. K. Hu, *Appl. Phys. Lett.* **72**, 1296 (1998).
- ¹³N. Tamura, J.-S. Chung, G.E. Ice, B.C. Larson, J.D. Budai, J.Z. Tischler, M. Yoon, E.L. Williams, and W.P. Lowe, *Mater. Res. Soc. Symp. Proc.*, **563** (1999) 175-80.
- ¹⁴N. Tamura, B. C. Valek, R. Spolenak, A. A. MacDowell, R. S. Celestre, H.A. Padmore, W. L. Brown, T. Marieb, J. C. Bravman, B. W. Batterman and J. R. Patel, *Mat. Res. Soc. Symp. Proc.*, **612** (2001) D.8.8.1 –D8.8.6
- ¹⁵R. Spolenak, D.L. Barr, M.E. Gross, K. Evans-Lutherodt, W.L. Brown, N. Tamura, A.A. MacDowell, R.S. Celestre, H.A. Padmore, J.R. Patel, B.C. Valek, J.C. Bravman, P. Flinn, T. Marieb, R.R. Keller, B.W. Batterman, *Mat. Res. Soc. Symp. Proc.*, **612** (2001) D10.3.1-D.10.3.7
- ¹⁶B.C. Valek, N. Tamura, R. Spolenak; A.A. MacDowell; R.S. Celestre; H.A. Padmore; J.C. Bravman; B.W. Batterman; J.R. Patel, *Mat. Res. Soc. Symp. Proc.* **673**, (2001) P7.7.1-P7.7.6
- ¹⁷B.C. Valek, N. Tamura, R. Spolenak, J.C. Bravman, A.A. MacDowell, R.S. Celestre, H.A. Padmore, W.L. Brown, B.W. Batterman and J.R. Patel, *Appl. Phys. Lett.* **81**, 4168-4170, (2002)
- ¹⁸R. Barabash, G.E. Ice, B.C. Larson, G.M. Pharr, K.-S. Chung, W. Yang, *Appl. Phys. Lett.*, **79**, 749, (2001)
- ¹⁹R. Barabash, G.E. Ice, F. Walker, *J. Appl. Physics*, accepted for publication in (2003)
- ²⁰D. Hughes and N. Hansen, *Acta Mater.* **48**, 2985-3004, (2000).
- ²¹Krivoglaz, M.A., *Theory of X-Ray and Thermal Neutron Scattering by Real Crystals*, Plenum Press, New York, 1969